EUROPEAN COMMISSION

HORIZON 2020 PROGRAMME - TOPIC H2020-LC-BAT-2020
Sodium-Ion and sodium Metal BAtteries for efficient and sustainable next-generation energy storage

GRANT AGREEMENT No. 963542

SIMBA – Deliverable Report

<< D3.2 – Operational in-situ NMR and SPM /first tests demonstration >>

Deliverable No.	SIMBA D3.2	
Related WP	WP3	
Deliverable Title	Operational in-situ NMR and SPM /first tests demonstration	
Deliverable Date	2021-12-31	
Deliverable Type	REPORT	
Dissemination level	Public (PU)	
Written By	Torsten Gutmann (TUDa) and Ying Zhan (TUDa)	2021-12-08
Checked by	Magdalena Graczyk-Zajac (TUDa)	2021-12-12
Reviewed by (if applicable)	Muhammad Abdelhamid (IFE) and Christian Jordy (SAFT)	2021-12-17
Approved by	Ralf Riedel (TUDa)	2021-12-20
Status	Final	2021-12-20

This project has received funding from the European Union's Horizon 2020 research and innovation programme under grant agreement No 963542.

Publishable summary

Monitoring structural changes in sodium/sodium ion battery systems during galvanostatic cycling is a challenging task that requires appropriate analytical techniques allowing the detection of structure moieties as a function of the time progress of the cycling process. A powerful technique that allows such analysis is in-situ solid-state NMR spectroscopy which can be applied to analyze local structural changes in alkali metal containing electrochemical cells. To perform such experiments appropriate cells have to be prepared which are stable during the cycling process. Furthermore, special in-situ NMR probes have to be set up that allow the measurement of solid-state NMR spectra under cycling conditions.

The successful preparation of electrochemical cells for in-situ solid-state NMR investigations is presented. For the model compounds LiCl and NaCl, as well as for electrochemical Li|$LiPF_6$|Li and Na|$NaPF_6$|Na cells the operational of the two single resonance channel probes (ATMC IN SITU NMR 300 and ATMC IN SITU NMR 600 WB) is shown. The obtained in-situ spectra allow the monitoring of structural changes in these cell systems. To obtain more details these experiments have to be combined with ex-situ NMR investigations that increase resolution.

Single particle measurement (SPM) is a powerful tool to investigate the electrochemical properties of a single particle of active material without considering the effect of the binder and conducting materials. It is employed in the SIMBA project to study the diffusion coefficients of sodium in the electrode, electrolyte and the charge transfer resistances across the electrode/electrolyte interface. The main processes of setting up the SPM device are detailed in this report. Besides, first measurements on a SiOC|$LiPF_6$|Li cell have been successfully performed to prove the operability of the SPM setup.

Contents

1 Purpose of the document 6
1.1 Document structure 6
1.2 Deviations from original description in the Grant Agreement Annex 1 Part A 6
1.2.1 Descriptions of work related to deliverable in GA Annex 1 – Part A 6
1.2.2 Time deviations from original planning in GA Annex 1 – Part A 6
1.2.3 Content deviations from original plan in GA Annex 1 – Part A 6
2 Introduction 7
3 In-situ solid-state NMR to identify structural changes in energy storage systems 8
3.1 Preparation of stable electrochemical cells for in-situ NMR 8
3.2 Operation of in-situ solid-state NMR equipment 8
3.2.1 Technical advances of the in-situ solid-state NMR equipment 8
3.2.2 Test of the in-situ solid-state NMR equipment on Li|$LiPF_6$|Li cell 10
3.2.3 Test of the in-situ solid-state NMR equipment on Na|$NaPF_6$|Na cell 11
4 Single particle measurement (SPM) 12
4.1 Setup of the single particle measurement 12
4.1.1 Microelectrode preparation 13
4.1.2 Electrochemical cell assembly 13
4.2 Test of the SPM equipment on SiOC|$LiPF_6$|Li cell 15
5 Conclusions and Recommendations 16
6 Risk Register 17
7 References 18
Appendix A - Table of Abbreviations 20
Appendix B - Acknowledgement 21
Appendix C - Disclaimer/Acknowledgement 22

Figure 1 a) Picture of a cylindrical 15 mm cell and the two parts of the cell as it was used to prepare stable cells for in-situ solid-state NMR investigations. b) Schematic illustration of the cell components (electrodes, separator on which the electrolyte is distributed) as used to prepare a metal|$NaPF_6$|metal cell. 8

Figure 2 Pictures of a) the 7 T NMR magnet system on which the ATMC IN SITU NMR 300 probe was installed, b) the probe connected to the SP-150 cycler system, and c) the cell as it is placed in this probe and the connections of the wires. 9

Figure 3 a) Static ^{23}Na solid-state NMR spectrum of NaCl obtained with the ATMC IN SITU NMR 300 probe at 7 T. b) Static ^{7}Li solid-state NMR spectrum of LiCl obtained with the ATMC IN SITU NMR 600 probe at 14 T. 9

Figure 4 Zoom in the range between 350 and 100 ppm of the ^{7}Li in-situ NMR spectra obtained for a Li|$LiPF_6$|Li cell when a current of 500 mA is applied for 15 h. 10

Figure 5 Zoom in the range between 1300 and 1000 ppm of the ^{23}Na in-situ NMR spectra obtained for a Na|$NaPF_6$|Na cell when a current of 500 mA is applied for 10 h. 11

Figure 6 Schematic illustration of a single particle measurement setup: potentiostat (left), electrochemical cell (middle) and microelectrode (right). 12

Figure 7 Main steps of setting up a single particle measurement 12

Figure 8 Main steps of preparing a microelectrode in the lab 13

Figure 9 Optical image of a single particle of SiOC ceramic under a microelectrode 13

Figure 10 Photo of a SiOC|$LiPF_6$|Li electrochemical cell used in single particle measurement 14

1 Purpose of the document

This document corresponds to D3.2 – Operational in-situ NMR and SPM /first tests demonstration. It aims to demonstrate the main steps of setting up the in-situ NMR and SPM equipment, including the results of the first measurements. This operation is shown for Li|$LiPF_6$|Li as well as Na|$NaPF_6$|Na cells.

1.1 Document structure

This document consists of three main parts:

Chapter 2 Introduction

Chapter 3 In-situ solid-state NMR to identify structural changes in energy storage systems

Chapter 4 Single particle measurement

1.2 Deviations from original description in the Grant Agreement Annex 1 Part A

1.2.1 Descriptions of work related to deliverable in GA Annex 1 – Part A

N/A.

1.2.2 Time deviations from original planning in GA Annex 1 – Part A

N/A.

1.2.3 Content deviations from original plan in GA Annex 1 – Part A

N/A.

2 Introduction

In a world of increasing digitization and the ongoing energy revolution, the market requires efficient electrochemical energy storage materials which can be applied in a sustainable way. Limited resources and material availability as well as missing recycling processes lead to an increased research focus on alternative materials which fulfil these requirements. Energy storage systems containing alkali metals seem to be highly efficient from the electrochemical point of view, however, the often used lithium-containing storage systems require lithium whose manufacturing is quite expensive since its abundance in earth crust is only 0,006 % which is widely distributed. An alternative is to substitute lithium by sodium which has a much higher abundance in the earth crust of 2.6 % and can be thus manufactured much easier. In the past few years, many efforts have been made in the field of sodium-containing energy storage materials [1–6]. Up to now, however, materials that can be used in many charging/discharging cycles, be produced cost-effectively as well as recycled and that fulfil security aspects are rare.

The overall goal of the SIMBA project aims to develop new materials for these purposes with the main focus on new electrode materials and solid electrolyte materials and their manufacturing. To optimize these novel materials in cell systems it is necessary to have specific analytical methods to enable the examination of processes such as ion transport and storage in electrode materials on the nanoscale under working conditions, i.e. during the charging and discharging process of the cell. A valuable tool to do this analysis is the use of ^{23}Na in-situ solid-state NMR which addresses changes in the local environment of sodium during the charging/discharging cycle. While in-situ solid-state NMR has been introduced for lithium battery research and applied many times [7–10], only a few examples (i.e. Gray and co-workers [11–13] and Gotoh and co-workers [14]) are known so far where studies have been performed on ^{23}Na using carbon materials as electrodes.

Single-particle measurement (SPM) is a novel technique, which is employed to evaluate the electrochemical properties of a single particle of active material without binder and conducting materials [15–17]. On account of that, insights into the intrinsic nature of the charge transport in the electrode material are provided, namely the charge transfer resistance and the minimum diffusion coefficient.

The first part of the report will describe how cells are prepared to perform ^{23}Na in-situ solid-state NMR measurements. Examples of standard cells that can be investigated with the in-situ setup are presented. Here the focus is on Li|$LiPF_6$|Li and Na|$NaPF_6$|Na cells to demonstrate the applicability of the setup to follow structural changes when a current is applied. In the second part, the main steps for setting up SPM equipment are demonstrated in detail. The lithium insertion and transport into silicon oxycarbide (SiOC) ceramic single particles (diameter of 10-25 µm) were tested and presented as an example.

3 In-situ solid-state NMR to identify structural changes in energy storage systems

3.1 Preparation of stable electrochemical cells for in-situ NMR

Before setting up the electrochemical in-situ solid-state NMR experiments, cells have to be prepared and their stability has to be tested by galvanostatic cycling experiments. Thus, the first task was to find a feasible way to handle the cell preparation. In Figure 1a, the typical cylindrical cell geometry as it can be used later for in-situ NMR experiments is shown. This cell contains two separable parts, in which the cell components (electrodes, separator on which the electrolyte is distributed etc.) can be placed before fixing the two parts together. In Figure 1b, a scheme of the cell components is shown as they were used to prepare a metal|electrolyte|metal cell. The preparation of the cells was performed in a glovebox under an argon atmosphere to prevent the cell components from contacting moisture and air.

a) b)

Figure 1 a) Picture of a cylindrical 15 mm cell and the two parts of the cell as it was used to prepare stable cells for in-situ solid-state NMR investigations. b) Schematic illustration of the cell components (electrodes, separator on which the electrolyte is distributed) as used to prepare a metal|$NaPF_6$|metal cell.

After assembling the cell components, the cell is ready for cycling experiments. In the first test runs, we produced standard Li|$LiPF_6$|Li and Na|$NaPF_6$|Na by fixing the wires to the electrode materials using commercial modelling clay provided by the NMR SERVICE. This was successful to obtain cells for proof-of-concept of the in-situ NMR setup. For the preparation of more complex cell systems, we had to change our strategy since the first test runs failed. Probably, the test cells were not sealed completely leading to reactions of the cell components with air or moisture causing cell decomposition tracked by a loss of the electrochemical properties in galvanostatic cycling experiments. This issue may be overcome by heating out all cell components in a vacuum drying oven and sealing the cells after preparation with cyanoacrylate glue.

3.2 Operation of in-situ solid-state NMR equipment

3.2.1 Technical advances of the in-situ solid-state NMR equipment

With the prepared electrochemical cells in hand, we started to set up the in-situ NMR experiments with the equipment provided by the NMR SERVICE company. The delivered equipment contains two single resonance channel probes (ATMC IN SITU NMR 300 and ATMC IN SITU NMR 600 WB) which enable the measurement of a large variety of NMR nuclei including ^{7}Li as well as ^{23}Na. Pictures of the 7 T NMR spectrometer system and the equipment for the in-situ experiments including the ATMC IN SITU NMR 300 probe as well as the cycler system and the placing of the cell in the probe are shown in Figure 2a-c.

a) b) c)

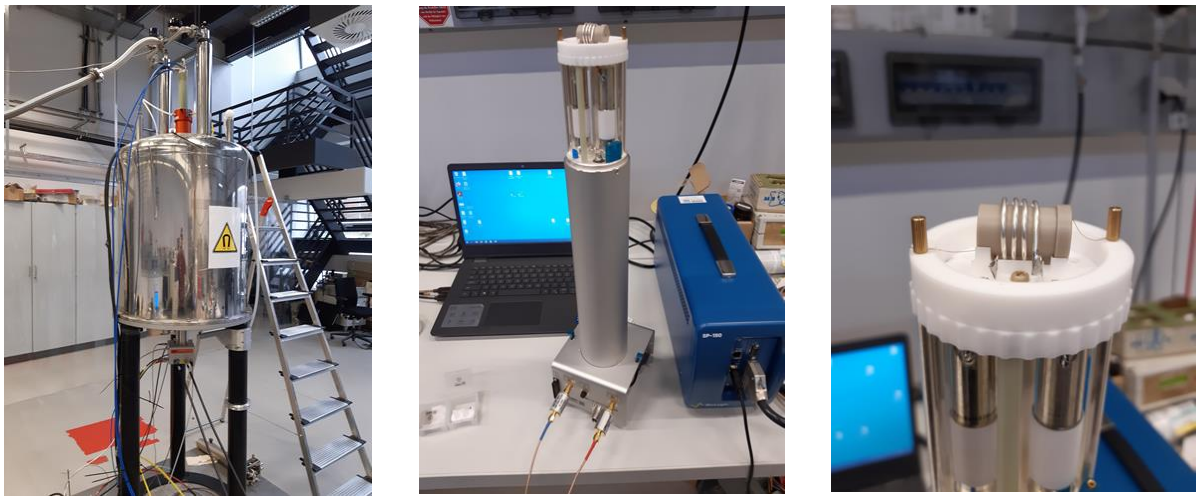

Figure 2 Pictures of a) the 7 T NMR magnet system on which the ATMC IN SITU NMR 300 probe was installed, b) the probe connected to the SP-150 cycler system, and c) the cell as it is placed in this probe and the connections of the wires.

The probes were installed on both, our 7 T and our 14 T magnet systems, respectively. To verify the operation of the probes static solid-state NMR spectra of ^{7}Li as well as of ^{23}Na on standard LiCl and NaCl samples, which were placed each in an empty cell, were recorded. These tests were successful on both spectrometers as shown for ^{23}Na in Figure 3a and ^{7}Li in Figure 3b demonstrating the basic operation of the probes. LiCl and NaCl are then later used to set the reference of the NMR spectra.

a) b)

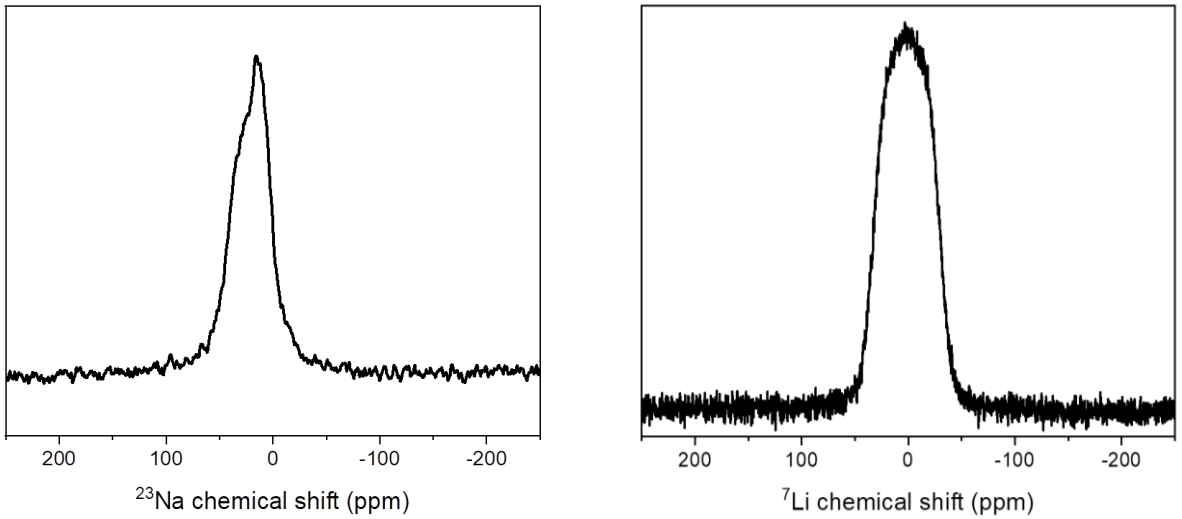

Figure 3 a) Static ^{23}Na solid-state NMR spectrum of NaCl obtained with the ATMC IN SITU NMR 300 probe at 7 T. b) Static ^{7}Li solid-state NMR spectrum of LiCl obtained with the ATMC IN SITU NMR 600 probe at 14 T.

In this context, the automatic tuning and matching available for these probes was tested to confirm their optimum operation. This is necessary since in the following in-situ NMR experiments it is required to address changes of the magnetic susceptibility of the samples during the galvanostatic

cycling that significantly affects the tuning and matching of the probe, and which has to be re-adjusted automatically during the in-situ NMR experiments. In order to implement the automatic matching/tuning procedure, a laboratory written program was used which performs this process after the recording of every single spectrum. This setup was then used to perform first in-situ NMR experiments on Li|$LiPF_6$|Li and Na|$NaPF_6$|Na cells on the 7 T magnet as described more in detail in sections 3.2.2 and 3.2.3. The 7 T magnet system was used for testing since it enables to perform also ex-situ measurements of the cell components at high spinning rates (up to 50 kHz) which is less practical on the 14 T magnet system due to occurrences of eddy currents that scale with the field strength.

3.2.2 Test of the in-situ solid-state NMR equipment on Li|$LiPF_6$|Li cell

After the basic setup of the in-situ NMR equipment, a standard Li|$LiPF_6$|Li cell was prepared according to the procedure described in section 3.1 and verify its ability to detect structural changes when a relatively high current of 500 mA is applied. This high value was used to obtain significant structural changes in the cell within a few hours, which is practical for operational proof of the setup. The results of these measurements are illustrated in Figure 4. All spectra show the typical signal at 245 ppm that refers to the lithium metal of the electrodes, respectively. Looking at the time dependence of the signal at 245 ppm it is visible that its intensity decreases significantly, which demonstrates that the content of lithium metal drops down when the current is applied. At the same time, a shoulder signal at 265 ppm which is close to the metal signal has appeared. This observation indicates that the environment of the formerly metallic lithium has changed. Compared with literature data [18] it is obvious that the lithium from the electrode forms dendritic structures leading to the obtained shoulder signal in the spectra.

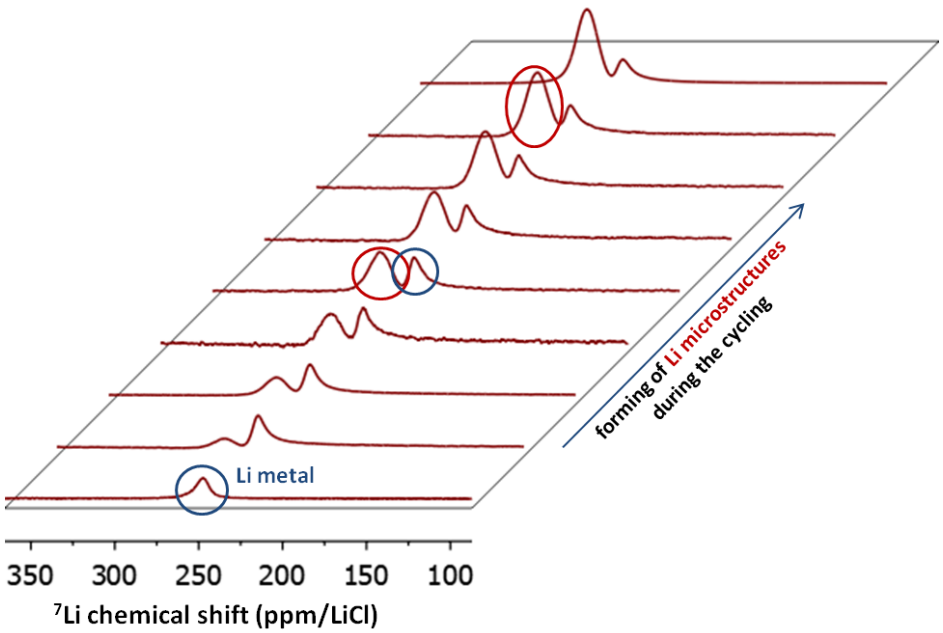

Figure 4 Zoom in the range between 350 and 100 ppm of the ^{7}Li in-situ NMR spectra obtained for a Li|$LiPF_6$|Li cell when a current of 500 mA is applied for 15 h.

3.2.3 Test of the in-situ solid-state NMR equipment on Na|$NaPF_6$|Na cell

After the suitability of the in-situ NMR setup was demonstrated on the lithium cell, we transferred our knowledge to investigate a sodium-containing cell similar to the lithium one. Here, a Na|$NaPF_6$|Na cell was prepared according to the procedure described in section 3.1. With the as-obtained cell, the in-situ solid-state NMR equipment was tested. Figure 5 shows the results of these measurements. Similar to the Li|$LiPF_6$|Li cell, a signal at 1135 ppm is obtained that refers to the sodium metal of the electrodes. When a current of 500 mA is applied to the cell for several hours, a significant decrease in intensity of the signal at 1135 ppm is observed while a shoulder signal at 1141 ppm near to the signal at 1135 ppm appeared. This observation indicates the formation of dendrites in the sodium cell where the chemical environment of the sodium metal has changed. This result clearly shows the similarities between lithium and sodium-containing cells. And this may help in future to explain NMR spectroscopic data obtained for sodium/sodium ion cells on the basic knowledge on lithium cells for which data is available.

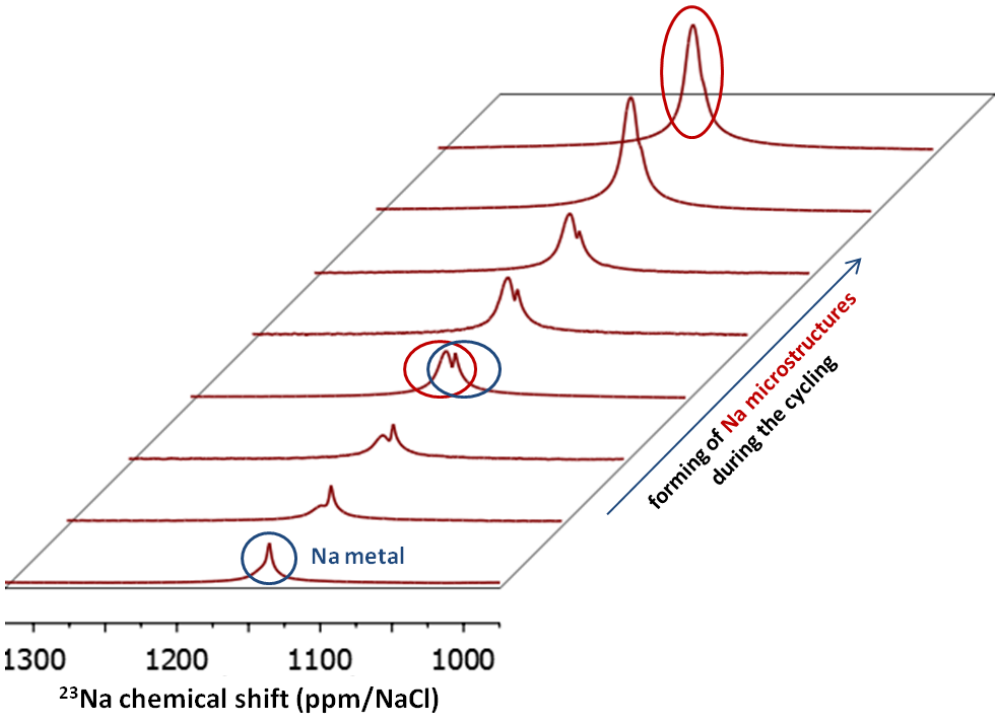

Figure 5 Zoom in the range between 1300 and 1000 ppm of the ^{23}Na in-situ NMR spectra obtained for a Na|$NaPF_6$|Na cell when a current of 500 mA is applied for 10 h.

4 Single particle measurement (SPM)

4.1 Setup of the single particle measurement

The schematic illustration of a single particle measurement setup is shown in Figure 6. A complete SPM setup consists of three main parts: i) microelectrode, ii) electrochemical cell, and iii) potentiostat. The main steps of setting up the SPM are presented in Figure 7 and detailed in the following subsections.

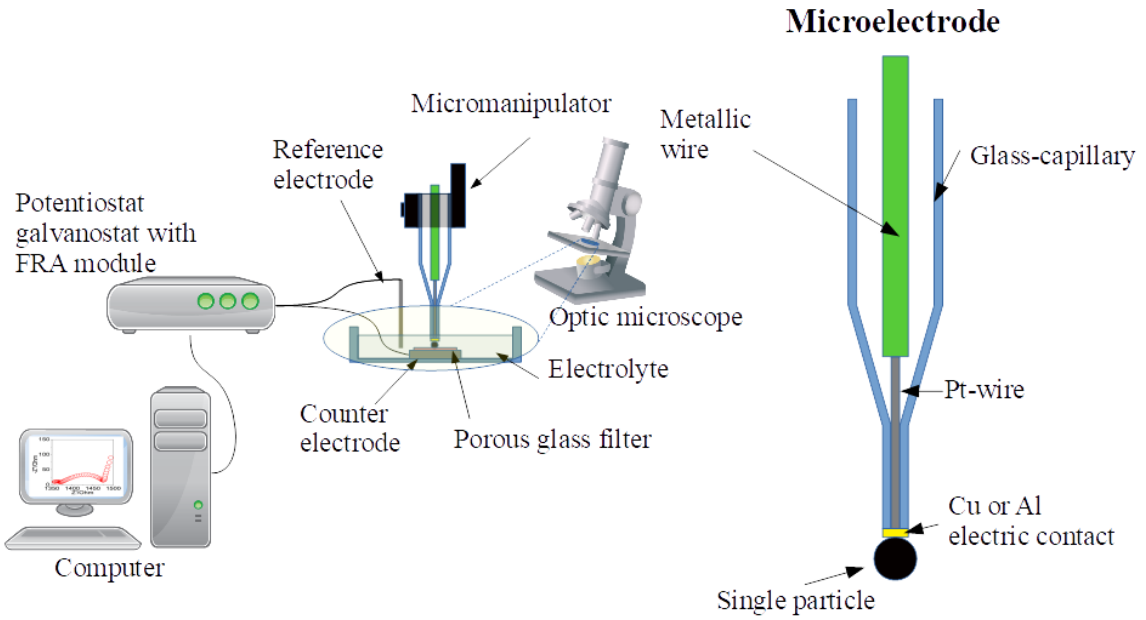

Figure 6 Schematic illustration of a single particle measurement setup: potentiostat (left), electrochemical cell (middle) and microelectrode (right).

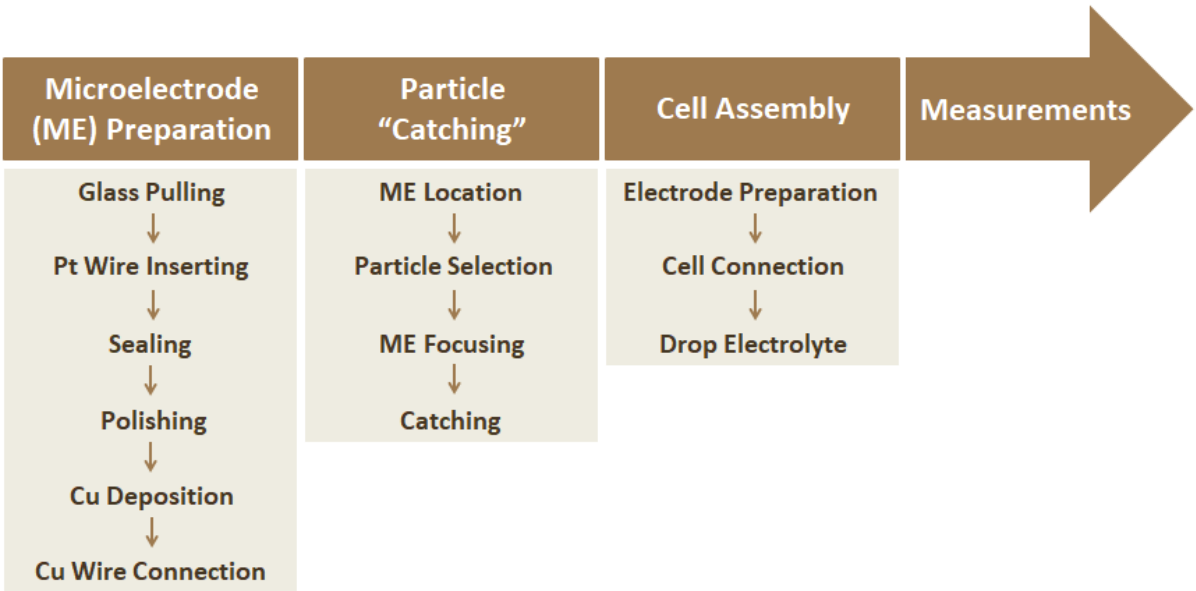

Figure 7 Main steps of setting up a single particle measurement

4.1.1 Microelectrode preparation

The microelectrode (ME) can be manufactured in the lab or purchased on the market. The main steps of preparing microelectrode in the lab are shown in Figure 8. A borosilicate glass capillary with an inner diameter of 0.58 mm is pulled by a Narishige PP-830 microelectrode puller to obtain two outer shells of the ME. A platinum wire with a diameter of 25 µm is inserted into the tip of the pulled glass capillary. The tip of the ME is subsequently sealed with a flame. In order to obtain good electric contact between the ME and the tested single particle, the tip of the ME is firstly polished and then electrodeposited with a thin film of copper by dipping the tip of the ME into an aqueous solution of 0.6 M $CuSO_4$ and 0.05 M H_2SO_4. Finally, a copper wire with a diameter of 200 µm is inserted and connected with the Pt wire. The ME is ready to use.

Figure 8 Main steps of preparing a microelectrode in the lab

4.1.2 Electrochemical cell assembly

The positioning setup for "catching" a particle and the components for assembling an electrochemical cell are placed in a glovebox to avoid the contamination of moisture and oxygen. The positioning system includes an inverted microscope and a micromanipulator, which is used to control the microelectrode to "catch" a particle with an ideal size of ca. 25 µm. As shown in Figure 9, after locating the ME on top of the selected single particle, the focus of the microscope should be changed to the shinning Cu-deposited Pt wire. The ME is gradually tuned to approach the single particle until both the ME and the particle are clearly visible under the microscope, which is considered to be a successful establishment of contact between the ME and the particle.

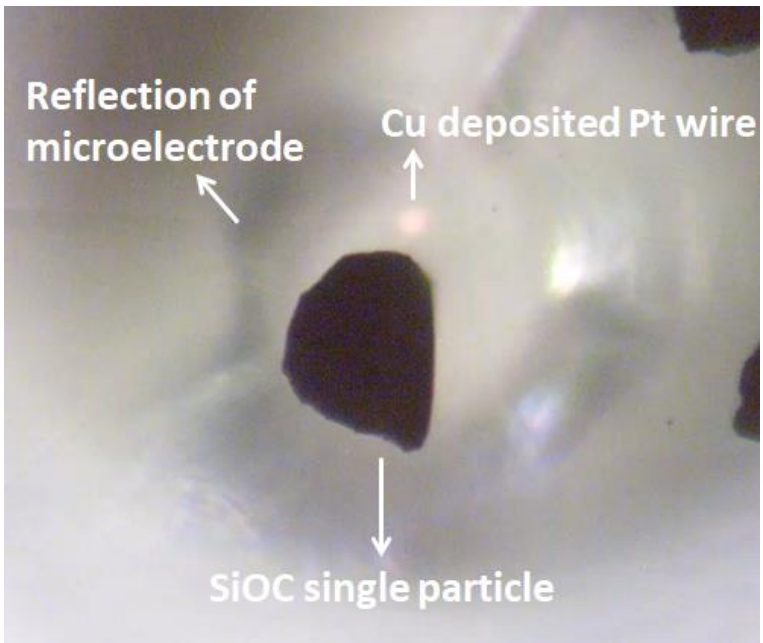

Figure 9 Optical image of a single particle of SiOC ceramic under a microelectrode

In the example shown in Figure 10, an electrochemical cell is assembled in the glovebox using Li strips as a reference and counter electrodes, and as an electrolyte 1 M $LiPF_6$ in EC:DMC (1:1) is dropped to cover these three electrodes. Due to the complexity of catching a single particle and assembling a cell in the glovebox, the mentioned steps in this subsection are the most challenging part of the single particle measurements.

The electrochemical cell is coupled with a potentiostat with the frequency response analysis (FRA) module and measurements with a very low current can be performed. The protocol of the evaluation of the measured data regarding the diffusion coefficients is described in D3.3.

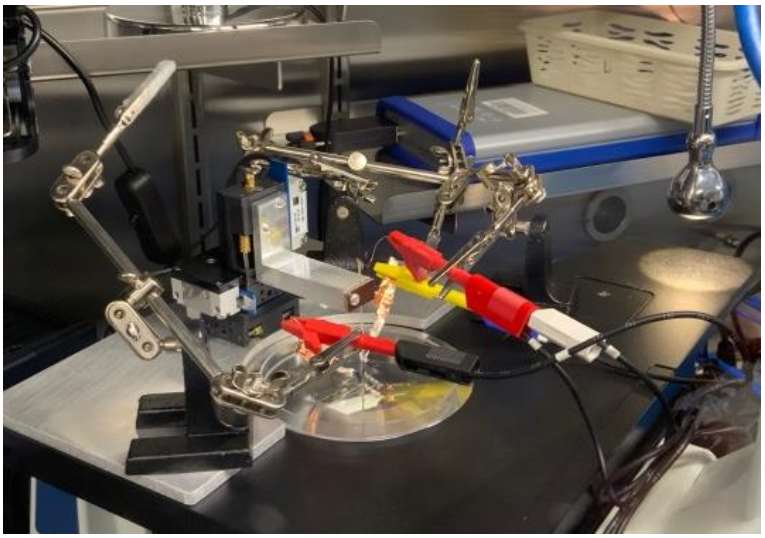

Figure 10 Photo of a SiOC|$LiPF_6$|Li electrochemical cell used in single particle measurement

4.2 Test of the SPM equipment on SiOC|$LiPF_6$|Li cell

As a test for the operability of the SPM setup, a SiOC|$LiPF_6$|Li electrochemical cell is prepared and measured following the aforementioned steps. Galvanostatic cycling is performed between 3.0 and 0.005 V at different currents. Figure 11a shows the delithiation curves of a single SiOC particle with a diameter of 12 µm measured with different currents. As the current increases from 5 nA to 50 nA, the delithiation capacity decreases from 0.89 nAh to 0.73 nAh. The cyclic voltammetry curves of a single SiOC particle (diameter of 10 µm) are shown in Fig. 11b. It is clear that the solid electrolyte interphase is formed on the surface of the SiOC from the electrochemical reduction of the electrolyte in the first cycle. The cyclic voltammetry curve of the second cycle corresponds well with the third cycle, indicating a stable structure of the electrode material.

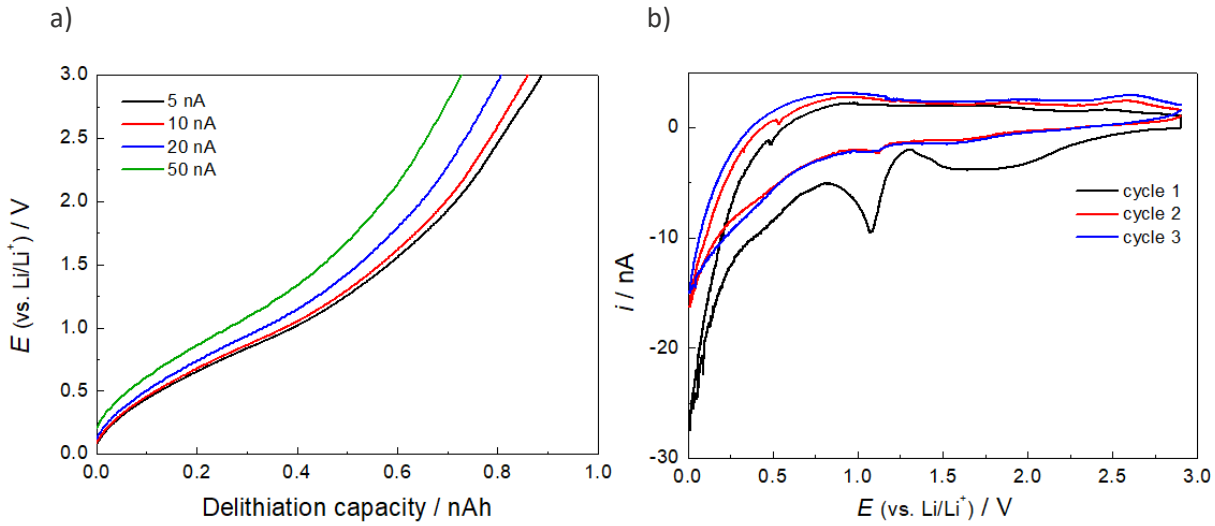

Figure 11 a) Delithiation curves of single SiOC particle (diameter of 12 µm) measured with different currents. b) Cyclic voltammetry curves of single SiOC particle (diameter of 10 µm).

5 Conclusions and Recommendations

The in-situ solid-state probes have been set up successfully at our 7 T and 14 T NMR magnet systems. The principle operation for solid-state NMR has been demonstrated on standard samples such as NaCl and LiCl. Furthermore, the operation of the automatic matching and tuning unit for in-situ NMR has been tested at 7 T for the cell systems Li|$LiPF_6$|Li and Na|$NaPF_6$|Na. Structural changes of the lithium respectively sodium environment in this cell during galvanostatic cycling has been monitored by in-situ solid-state NMR where significant changes of the signal of metallic sodium suggested the formation of dendrites during the cycling process.

The presented results let us assume that our approach can be transferred in future to interesting cell systems containing sodium/sodium ions especially those, that contain solid electrolytes and novel electrode materials as developed in WP 2. Furthermore, structural changes that may affect the long-time stability of novel cells can be analyzed by our approach. In future, we will also analyze the effect of temperature on structural changes of sodium environments in such cells that may help to optimize the cell composition for a larger temperature range.

The main steps of setting up the single particle measurement setup have been demonstrated and will be applied as a protocol for further SPM investigation in the SIMBA project. The trial test of SPM setup on a SiOC|$LiPF_6$|Li cell has been successfully performed. The experience of these first experiments will be transferred to investigate the Na^+ transport properties in the electrode materials synthesized in WP2.

6 Risk Register

Risk No.	What is the risk	Probability of risk occurrence[1]	Effect of risk[2]	Solutions to overcome the risk
WP3.4	Signals in the ^{23}Na in-situ solid-state spectra measured under static conditions can be quite broad and thus in some cases may not be detectable especially when the amount of sodium is low and the quadrupolar coupling is large.	2	3	A combination of in-situ with high-resolution ex-situ measurements at high spinning frequencies of 50 kHz may overcome resolution issues. Cell geometries for ^{23}Na in-situ NMR containing higher sodium content have to be designed.
WP3.5	Too soft electrodes materials (e.g. some carbonaceous materials) are difficult to be immobilized at the top of the microelectrode	2	2	Softer electrode material (Coating with aluminium instead of copper) and bigger surface of the electrodes will used instead

[1] Probability risk will occur: 1 = high, 2 = medium, 3 = Low

[2] Effect when risk occurs: 1 = high, 2 = medium, 3 = Low

7 References

[1] K.B. Hueso, M. Armand, T. Rojo, High temperature sodium batteries: status, challenges and future trends, Energy Environ. Sci. 6 (2013) 734. https://doi.org/10.1039/c3ee24086j.

[2] N. Yabuuchi, K. Kubota, M. Dahbi, S. Komaba, Research development on sodium-ion batteries, Chem. Rev. 114 (2014) 11636–11682. https://doi.org/10.1021/cr500192f.

[3] C. Jiang, Y. Fang, W. Zhang, X. Song, J. Lang, L. Shi, Y. Tang, A Multi-Ion Strategy towards Rechargeable Sodium-Ion Full Batteries with High Working Voltage and Rate Capability, Angew. Chem. 130 (2018) 16608–16612. https://doi.org/10.1002/ange.201810575.

[4] I. Landa-Medrano, C. Li, N. Ortiz-Vitoriano, I. Ruiz de Larramendi, J. Carrasco, T. Rojo, Sodium-Oxygen Battery: Steps Toward Reality, J. Phys. Chem. Lett. 7 (2016) 1161–1166. https://doi.org/10.1021/acs.jpclett.5b02845.

[5] H. Wang, E. Matios, J. Luo, W. Li, Combining theories and experiments to understand the sodium nucleation behavior towards safe sodium metal batteries, Chem. Soc. Rev. 49 (2020) 3783–3805. https://doi.org/10.1039/D0CS00033G.

[6] B. Sun, P. Xiong, U. Maitra, D. Langsdorf, K. Yan, C. Wang, J. Janek, D. Schröder, G. Wang, Design Strategies to Enable the Efficient Use of Sodium Metal Anodes in High-Energy Batteries, Adv. Mater. 32 (2020) e1903891. https://doi.org/10.1002/adma.201903891.

[7] C.P. Grey, J.M. Tarascon, Sustainability and in situ monitoring in battery development, Nat. Mater. 16 (2017) 45–56. https://doi.org/10.1038/NMAT4777.

[8] X. Liu, Z. Liang, Y. Xiang, M. Lin, Q. Li, Z. Liu, G. Zhong, R. Fu, Y. Yang, Solid-State NMR and MRI Spectroscopy for Li/Na Batteries: Materials, Interface, and In Situ Characterization, Advanced Materials (2021). https://doi.org/10.1002/adma.202005878.

[9] S. Krachkovskiy, M.L. Trudeau, K. Zaghib, Application of Magnetic Resonance Techniques to the In Situ Characterization of Li-Ion Batteries: A Review, Materials 13 (2020). https://doi.org/10.3390/ma13071694.

[10] M. Mohammadi, A. Jerschow, In situ and operando magnetic resonance imaging of electrochemical cells: A perspective, Journal of Magnetic Resonance 308 (2019). https://doi.org/10.1016/j.jmr.2019.106600.

[11] O. Pecher, P.M. Bayley, H. Liu, Z. Liu, N.M. Trease, C.P. Grey, Automatic Tuning Matching Cycler (ATMC) in situ NMR spectroscopy as a novel approach for real-time investigations of Li- and Na-ion batteries, J. Magn. Reson. 265 (2016) 200–209. https://doi.org/10.1016/j.jmr.2016.02.008.

[12] P.M. Bayley, N.M. Trease, C.P. Grey, Insights into Electrochemical Sodium Metal Deposition as Probed with in Situ (23)Na NMR, J. Am. Chem. Soc. 138 (2016) 1955–1961. https://doi.org/10.1021/jacs.5b12423.

[13] J.M. Stratford, P.K. Allan, O. Pecher, P.A. Chater, C.P. Grey, Mechanistic insights into sodium storage in hard carbon anodes using local structure probes, Chem. Commun. (Camb) 52 (2016) 12430–12433. https://doi.org/10.1039/c6cc06990h.

[14] K. Gotoh, T. Yamakami, I. Nishimura, H. Kometani, H. Ando, K. Hashi, T. Shimizu, H. Ishida, Mechanisms for overcharging of carbon electrodes in lithium-ion/sodium-ion batteries analysed by operando solid-state NMR, J. Mater. Chem. A 8 (2020) 14472–14481. https://doi.org/10.1039/D0TA04005C.

[15] D.W. Dees, K.G. Gallagher, D.P. Abraham, A.N. Jansen, Electrochemical Modeling the Impedance of a Lithium-Ion Positive Electrode Single Particle, J. Electrochem. Soc. 160 (2013) A478–A486. https://doi.org/10.1149/2.055303jes.

[16] J. Lim, Y. Li, D.H. Alsem, H. So, S.C. Lee, P. Bai, D.A. Cogswell, X. Liu, N. Jin, Y.S. Yu, N.J. Salmon, D.A. Shapiro, M.Z. Bazant, T. Tyliszczak, W.C. Chueh, Origin and hysteresis of lithium compositional spatiodynamics within battery primary particles, Science (80-.). 353 (2016) 566–571. https://doi.org/10.1126/science.aaf4914.

[17] H. Munakata, B. Takemura, T. Saito, K. Kanamura, Evaluation of real performance of $LiFePO_4$ by using single particle technique, J. Power Sources. 217 (2012) 444–448. https://doi.org/10.1016/j.jpowsour.2012.06.037.

[18] R. Bhattacharyya, B. Key, H. Chen, A.S. Best, A.F. Hollenkamp, C.P. Grey, In situ NMR observation of the formation of metallic lithium microstructures in lithium batteries, Nat. Mater. 9 (2010) 504–510. https://doi.org/10.1038/nmat2764.

Appendix A - Table of Abbreviations

Symbol / Shortname	
FRA	Frequency Response Analysis
MAS	Magic Angle Spinning
ME	Microelectrode
NMR	Nuclear Magnetic Resonance
SPM	Single Particle Measurement

Appendix B - Acknowledgement

The author(s) would like to thank the partners in the project for their valuable comments on previous drafts and for performing the review.

Project partners:

#	Partner	Partner Full Name
1	TUDa	TECHNISCHE UNIVERSITAT DARMSTADT
2	UU	UPPSALA UNIVERSITET
3	UBham	THE UNIVERSITY OF BIRMINGHAM
4	WMG	THE UNIVERSITY OF WARWICK
5	KIT	KARLSRUHER INSTITUT FUER TECHNOLOGIE
6	CEA	COMMISSARIAT A L ENERGIE ATOMIQUE ET AUX ENERGIES ALTERNATIVES
7	IFE	INSTITUTT FOR ENERGITEKNIKK
8	SAS	USTAV ANORGANICKEJ CHEMIE SLOVENSKA AKADEMIA VIED (Institute of Inorganic Chemistry, Slovak Academy of Sciences)
9	FHG	FRAUNHOFER GESELLSCHAFT ZUR FOERDERUNG DER ANGEWANDTEN FORSCHUNG E.V.
10	JM	JOHNSON MATTHEY PLC
11	Elkem	ELKEM AS
12	YUN	YUNASKO-UKRAINE LLC
13	SAFT	SAFT
14	Altris	ALTRIS AB
15	Recupyl	TES RECUPYL SAS
	UNR	UNIRESEARCH BV

Appendix C - Disclaimer/Acknowledgement

This project has received funding from the European Union's Horizon 2020 research and innovation programme under grant agreement No 963542. The information and views set out in this publication does not necessarily reflect the official opinion of the European Commission. Neither the European Union institutions and bodies nor any person acting on their behalf, may be held responsible for the use which may be made of the information contained therein.